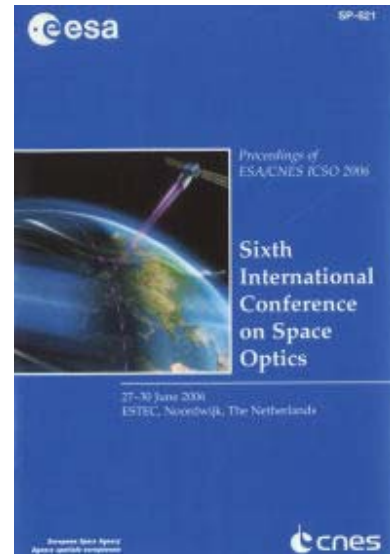


# International Conference on Space Optics—ICSO 2006

Noordwijk, Netherlands

27–30 June 2006

*Edited by Errico Armandillo, Josiane Costeraste, and Nikos Karafolas*



## *Developments of capacitance stabilised etalon technology*

*R. A. Bond, M. Foster, C. Thwaite, C. K. Thompson, et al.*



## DEVELOPMENTS OF CAPACITANCE STABILISED ETALON TECHNOLOGY

R. A. Bond<sup>(1)</sup>, M. Foster<sup>(2)</sup>, C. Thwaite<sup>(1)</sup>, C. K. Thompson<sup>(1)</sup>, D. Rees<sup>(2)</sup>, I.V. Bakalski<sup>(2)</sup> and J. Pereira Do Carmo<sup>(3)</sup>

<sup>(1)</sup> ABSL, Culham Science Centre, Abingdon, Oxon, UK, [robert.bond@absl.co.uk](mailto:robert.bond@absl.co.uk):

<sup>(2)</sup> Hovemere Ltd, Arctic House, Rye Lane, Dunton Green, Sevenoaks, TN14 5HD, UK, [mfoster@hovemere.co.uk](mailto:mfoster@hovemere.co.uk):

<sup>(3)</sup> ESTEC, Keplerlaan 1, P O Box 299, 2200 AG Noordwijk ZH, The Netherlands, [Joao.Pereira.Do.Carmo@esa.int](mailto:Joao.Pereira.Do.Carmo@esa.int):

### ABSTRACT

This paper describes a high-resolution optical filter (HRF) suitable for narrow bandwidth filtering in LIDAR applications. The filter is composed of a broadband interference filter and a narrowband Fabry-Perot etalon based on the capacitance stabilised concept.

The key requirements for the HRF were a bandwidth of less than 40 pm, a tuneable range of over 6 nm and a transmission greater than 50%. These requirements combined with the need for very high out-of-band rejection (greater than 50 dB in the range 300 nm to 1200 nm) drive the design of the filter towards a combination of high transmission broadband filter and high performance tuneable, narrowband filter.

### 1. INTRODUCTION

A key element of any LIDAR instrument is the optical filtering system that is used to spectrally filter the incoming light. For LIDAR applications, including wind and aerosol measurements, spectral filtering is used to separate the narrow aerosol Mie back-scattered signal from the molecular Rayleigh back-scattered signal. For LIDAR applications using the DIAL method (to measure water vapour and CO<sub>2</sub> concentrations, for example), spectral filtering is necessary in order to separate the return signals from the multiple laser pulses. In addition, narrow-band filtering is essential in reducing the affect of background radiation on the observed signal-to-noise ratio that might otherwise overwhelm the back-scattered LIDAR signal, particularly during daytime.

Two particular applications that would require narrow-bandwidth spectral filtering are firstly the Space-borne DIAL LIDAR proposed for the ESA WALES (Water Vapour Lidar Experiment in Space) mission and secondly, the Space-borne ATLID Lidar. The primary objective of the WALES mission is to study the water vapour distribution in the lower atmosphere. The primary objective of ATLID (as a critical part of the EarthCARE Mission) is the measurement of aerosols, cloud and atmospheric properties relating to Energy Transfer within the troposphere and low stratosphere.

The development and demonstration of a new high performance optical filter with narrow bandwidth (i.e. the HRF) is essential for these applications, in order to provide sufficient background rejection and avoid unacceptable reduction in the signal-to-noise ratio.

### 2. THE HRF DESIGN

#### 2.1. DESIGN TRADE-OFFS

The design of the High-Resolution Filter is driven by the combined requirements of narrow bandwidth and large free spectral range (spectral separation of transmission fringes). Achieving these two parameters concurrently is difficult and greatly restricts the choice of filter technology, particularly in view of the high transmission required. After performing a detailed trade-off of available filter technologies, the Fabry-Perot étalon was selected as the principal narrowband filter element, augmented by an interference filter for broadband rejection.

## 2.2 THE HRF ASSEMBLY

The two filter elements of the HRF are incorporated in a mechanical structure and illuminated by collimated light delivered via a fibre-optic and collimating lens assembly (see Figure 1 and 2). After traversing the filter system, the light is focused onto a primary exit fibre-optic and transmitted to a detector for analysis. A secondary exit provides a means of calibrating the signal intensity.

The internal configuration of the HRF can be seen in the sectional view of Figure 1.

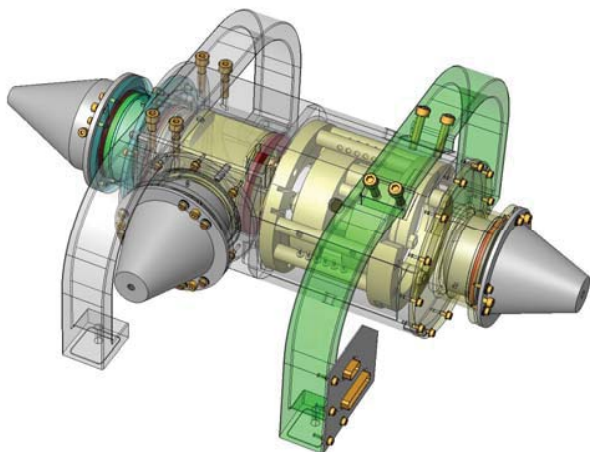


Figure 1: The High-Resolution Optical Filter (HRF).

## 2.3 THE BROADBAND FILTER

Broadband filtering is achieved via a high performance, commercially available, interference filter with the following specification:

- Bandwidth: 2 nm (FWHM)
- Transmission: > 80 %
- Blocking range: > 50 dB (300 nm to 1200 nm)

The interference filter was supplied by Barr Associates in the USA.

## 2.4 THE CAPACITANCE-STABILISED FABRY-PEROT ETALON

Narrowband filtering is achieved using a Capacitance-Stabilised Fabry-Perot étalon. A Capacitance-Stabilised étalon [1] (CSE) utilises three spacers, comprised of stacks of piezo-electric transducer elements, to adjust the

separation of the étalon plates and hence provide tuneability. In addition, the ability to separately control each of the spacers allows the plate parallelism to be adjusted, a capability that is not present in other Fabry-Perot étalon designs (for example fixed-spacer).

The CSE also incorporates three capacitor elements acting as proxies for the length of the spacers containing the transducers. By means of a feedback circuits, these enable the plate parallelism and separation always to be precisely controlled and maintained. The feedback control is implemented using a capacitance bridge technique [1] which assures precise control of the étalon at all times, with time-constants of less than 1 ms.

The CSE has been extensively tested and used in a large number of optical systems over the past 20 years, giving excellent optical performance and reliability. CSEs have been successfully flown on the NASA UARS [2] mission and have also been taken through full engineering-level vibration testing as part of the NASA GLAS project [3]. The overall configuration of the HRF is shown in Figure 2.

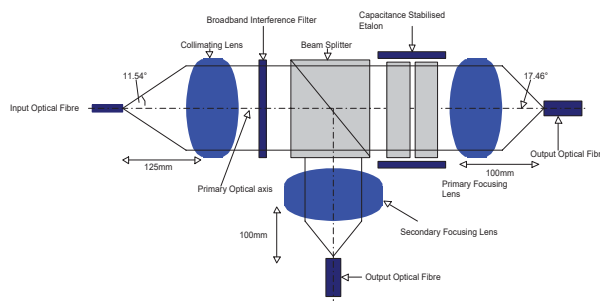


Figure 2: The Optical Configuration of the HRF.

## 2.5 THERMO-MECHANICAL DESIGN

The key design drivers for the mechanical design of the HRF are:

- To provide a structure which is stiff and stable to accurately locate the optical components.
- To provide a structure that protects the optical components from vibration during operation and during on-ground testing, including environmental testing.
- To minimise mass.

- To provide a structure which is insensitive to the thermal environment (i.e. accepts a large range of environment temperatures and temperature gradients).

In the HRF, these requirements are met by the following design features:

- The CSE is housed within a large tube (the CSE tube) that also houses a sub-assembly containing the interference filter and the beam splitter.
- The three lens assemblies are mounted within conical structures that are mounted onto the CSE tube.
- Doweled flanged joints on these structures provide rigid and precise mechanical connection / alignment.
- The CSE tube is mounted on two “goal post” support legs that provide vibration and thermal isolation of the main assembly.

### 3. MODELLED PERFORMANCE

#### 3.1. THEORETICAL PERFORMANCE

The performance of the HRF is largely dependent on the performance of the Capacitance-Stabilised Etalon (CSE). The key performance parameters of the CSE are the transmission and bandwidth together with the free spectral range. The bandwidth and free spectral range of an étalon are related by its *finesse*, which is a measure of the degree of interference between light rays reflected between the two étalon plates. The requirements of small bandwidth, large free spectral range and high transmission imply high values of reflective and overall finesse.

The overall finesse is dependent on several contributions each of which depends on a particular characteristic of the étalon plates and optical configuration. The overall finesse is expressed approximately by Eq. 1.

$$\frac{1}{F^2} \approx \frac{1}{F_D^2} + \frac{1}{F_R^2} + \frac{1}{F_A^2} \quad (1)$$

where  $F_D$  is the defect finesse,  $F_R$  is the reflective finesse and  $F_A$  is the aperture finesse.

The target finesse for the HRF CSE is 150. This is a demanding requirement and necessitates a minimum defect finesse of 200. This is equivalent to a plate flatness of  $\lambda/280$  (measured at  $\lambda = 633$  nm). In order to allow for some margin, it has been necessary to manufacture the HRF CSE étalon plates to a flatness of  $\lambda/300$  at 633 nm (corresponding to a defect finesse of 220 at 935.5 nm).

The reflective finesse is determined by the reflectivity of the étalon plates and increases with plate reflectivity. However, as the reflectivity is increased the transmission decreases and the optimum choice of plate reflectivity is a trade-off between achieving the required overall finesse and transmission. This trade-off is shown in the graphs of Figure and Figure .

Using the above trade-off analysis, an optimum reflectivity of 98.8% was selected. This value allows both the required high overall finesse and high transmission to be achieved.

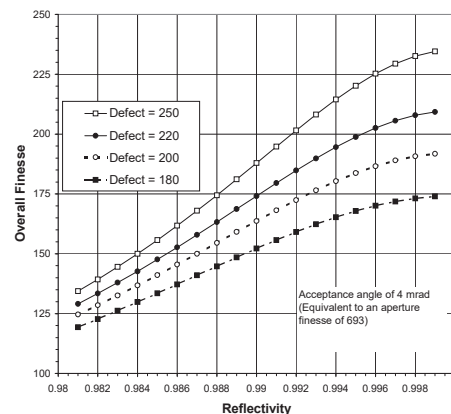


Figure 3: The overall finesse of the CSE as a function of plate reflectivity.

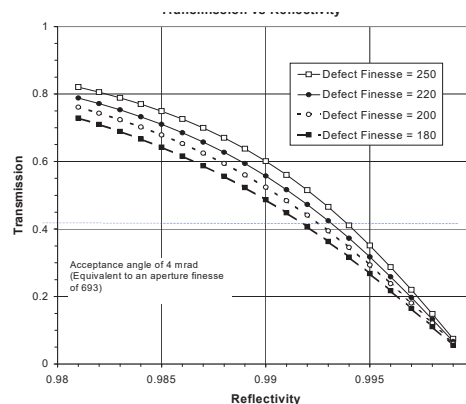


Figure 4: The transmission of the CSE as a function of plate reflectivity.

It should be noted that the aperture finesse (the third contribution to Eq. 1) is a function of the number of orders,  $n$ , and the acceptance angle,  $\theta$ , which in turn is dependant on the optical configuration of the collimating lens system. For the HRF system, the aperture finesse is high ( $> 600$ ) and is, therefore, less important in optimising the system performance.

Although the finesse is important in determining the bandwidth, on its own it does not uniquely define it. This is because bandwidth and free spectral range can be interchanged whilst maintaining the same finesse. However, in a system containing both a broadband and narrowband filter there is a minimum free spectral range that minimises the amount of out-of-band radiation whilst minimising the bandwidth. This minimum free spectral range can be determined using the so-called *filtrage*,  $FT$ , defined by Eq. 2.

$$FT = \frac{\int_a^b T(\theta, \lambda) \delta\lambda}{\int_{-\infty}^{\infty} T(\theta, \lambda) \delta\lambda} \quad (2)$$

where  $a$  is the lower bound of the central region (or FWHM) and  $b$  is the upper. Analysis based on the filtrage gives an optimum free spectral range of 4 nm for the HRF CSE.

Finally, based on the optimised parameters the transmission function of the CSE is shown in Figure 5.

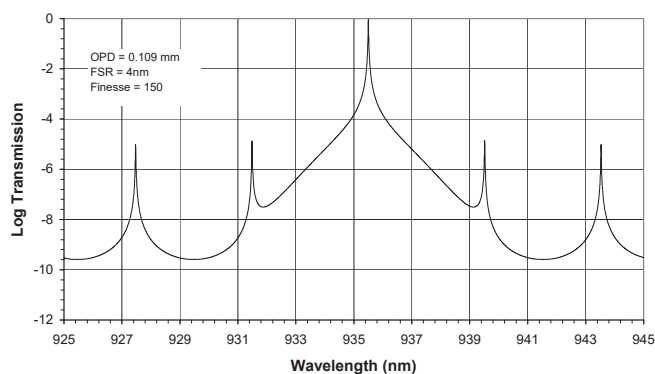


Figure 5: The Transmission function of the HRF filter train (CSE and interference filter) over a 20 nm range.

The CSE performance parameters are summarised in the Table 1.

Table 1: Predicted CSE optical performance parameters.

Parameter	Value
Aperture	50 mm
Free spectral range	4 nm
Reflectivity	98.8 % $\pm$ 0.2
Plate flatness (target)	$\lambda/300 \pm 20$
Defect Finesse	220
Overall Finesse	160 $\pm$ 12
Bandwidth	25 $\mu$ m $\pm$ 2 $\mu$ m
Transmission	64 % $^{+4}_{-7}$
Tuning Range	9 nm
Tuning Resolution	2.5 $\mu$ m

### 3.2. THERMO-MECHANICAL PERFORMANCE

The structural philosophy of the HRF design is to combine the high stiffness of the tube assembly (where all natural frequencies would be greater than about 600 Hz) with the relative flexibility of the legs (which would give natural frequencies for the assembly in the range of 100 to 300 Hz) to simultaneously satisfy the stringent optical accuracy and vibration environment requirements. A spin-off advantage of this “stiff-on-flexible” approach is that the designs of the tubes and the legs are decoupled.

The optimum choice of leg resonant frequency depends on the HRF vibration response to the three environment inputs, namely: sine vibration, shock and random vibration. For a single degree-of-freedom system this is illustrated in Figure . It shows that ideally, the structural frequencies should be in the range 150-250 Hz, as this gives the minimum overall response.

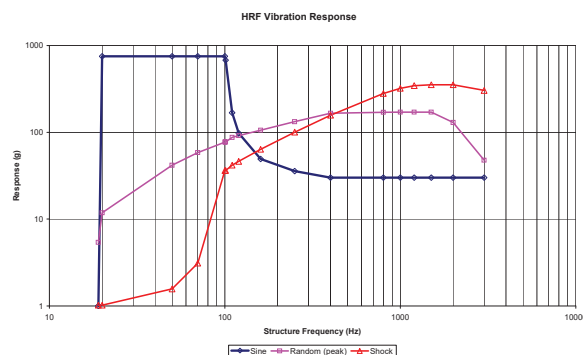


Figure 6: HRF Single DoF system responses (variation of peak responses with structural frequency).

#### 4. MANUFACTURE AND TESTING

This section describes in more detail the manufacture and testing of the HRF.

Figure 7 shows the CSE mounted in its cage, with the internal electrical wiring to the PZT transducers and capacitor elements.

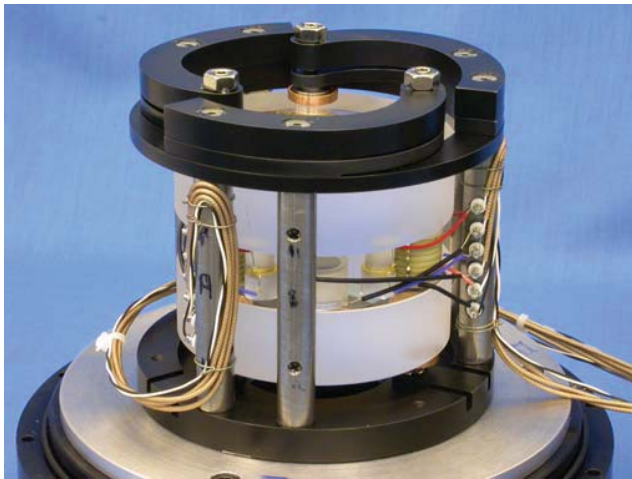


Figure 7: The HRF CSE mounted in its cage;

Figure 8 shows the mechanical tubular structure within which the CSE is mounted.



Figure 8: The HRF mechanical mounting structure.

The performance of the CSE itself was tested both in an imaging and filter mode of operation, prior to integration within the complete HRF optical system and its mechanical structure.

The HRF filter was initially tested in a filter configuration with the fringes projected onto a CCD camera. Due to the large FSR of the filter

only part of one fringe could be observed. Since the étalon uses piezo-electric transducers to enable the optical path difference to be actively controlled, the CSE spacing was adjusted using these elements in order to demonstrate its tuning capabilities and to measure its free spectral range in tuning step space.

A full scan of the HRF transmission function is shown in Fig. 9. The results displayed in these figure demonstrate that the filter bandwidth is a  $\sim 32$  pm and the free spectral range is 4 nm, corresponding to a finesse of  $\sim 125$ .

The total tunable range of the HRF is 8.4 nm, slightly more than 2 FSR at 935 nm.

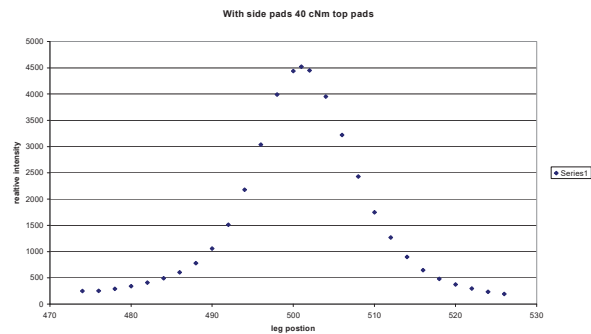


Figure 9: Optical performance of the HRF filter: This figure shows the transmission function of the filter.

The imaged fringe is shown below in Fig. 10.

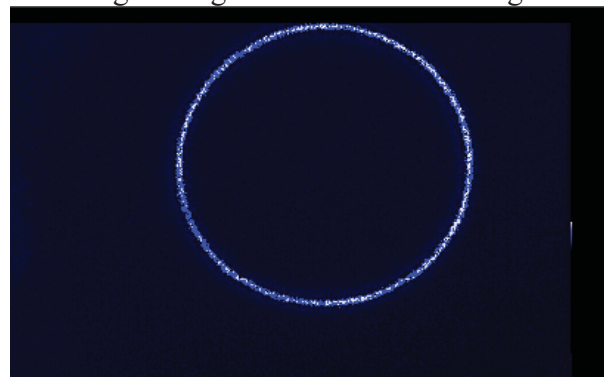


Figure 10. This shows an image of the Fabry Perot fringes. The filter bandwidth is 32 pm with a peak transmission of 55 %.

The CSE was then placed in a collimated beam and the light passing through the filter was focused onto the output optic fibre. The intensity of the light passing through the

system was monitored as the etalon was stepped through its complete tuning range.

The transmission function of the filter is displayed in Fig. 11.

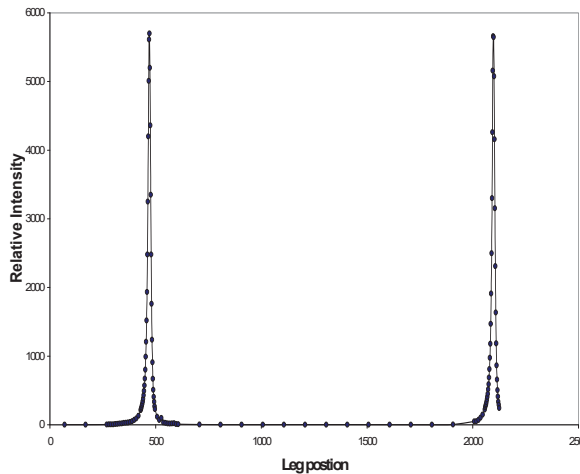


Figure 11: The Transmission Function of the HRF

Table 2: The measured performance of the HRF

Parameter	Value
OPD	109 $\mu\text{m}$
FSR	4 nm
Finesse	125
Working Aperture	50 mm
Tuning range	> 8 nm
Tuning resolution	2.4 $\mu\text{m}$
Linearity	< $10^{-3}$
Reflectivity	98.67 %
Defect finesse (@ 935 nm)	> 180
Parallelism	$\lambda/800$
Transmission	55 %
<b>Mounting condition</b>	
Side pad torque	10 cNm

## Conclusions

The paper has presented the design of a high performance optical filter based on a combination of a narrowband Capacitance-Stabilised Etalon and a broadband interference filter. The design includes a mechanical structure which houses the optical components within stiff tubes and isolates them from the environment via flexible legs.

The CSE demonstrated an overall finesse of 125 with a corresponding transmission of 55 %. This represents a matching plate flatness of

<  $\lambda/280$  @ 633 nm over the working aperture of the etalon. Additionally the tuning range of the filter has been shown to be greater than 8 nm with a FSR of 4 nm.

The demonstrated performance represents the state-of-the-art in terms of Fabry-Perot technology. Achieving such a high level of defect finesse over a 50 mm aperture will lead to significant gains in the detection chain of LIDAR instruments and help reduce the complexity of these systems.

## References

1. Rees D., I. McWhirter, P.B. Hays and T. Dines, (1981). A Stable, Rugged, Capacitance-stabilized Piezoelectric Scanned Fabry-Perot Etalon. J. Phys. E: Sci. Instrum. 14, 1320-1325.
2. Skinner W.R., P.B. Hays, and V.J. Abreu., Optimisation of a triple étalon interferometer, Appl. Opt. 26, 2817-2827, 1987.
3. McKay J.A. and D. Rees, "Space Qualified Etalon" Opt. Eng. 39(1) 315-319, (2000).